ESO219-024 (IRAS13025-4911)

A Seyfert II Galaxy SBc(B) ...

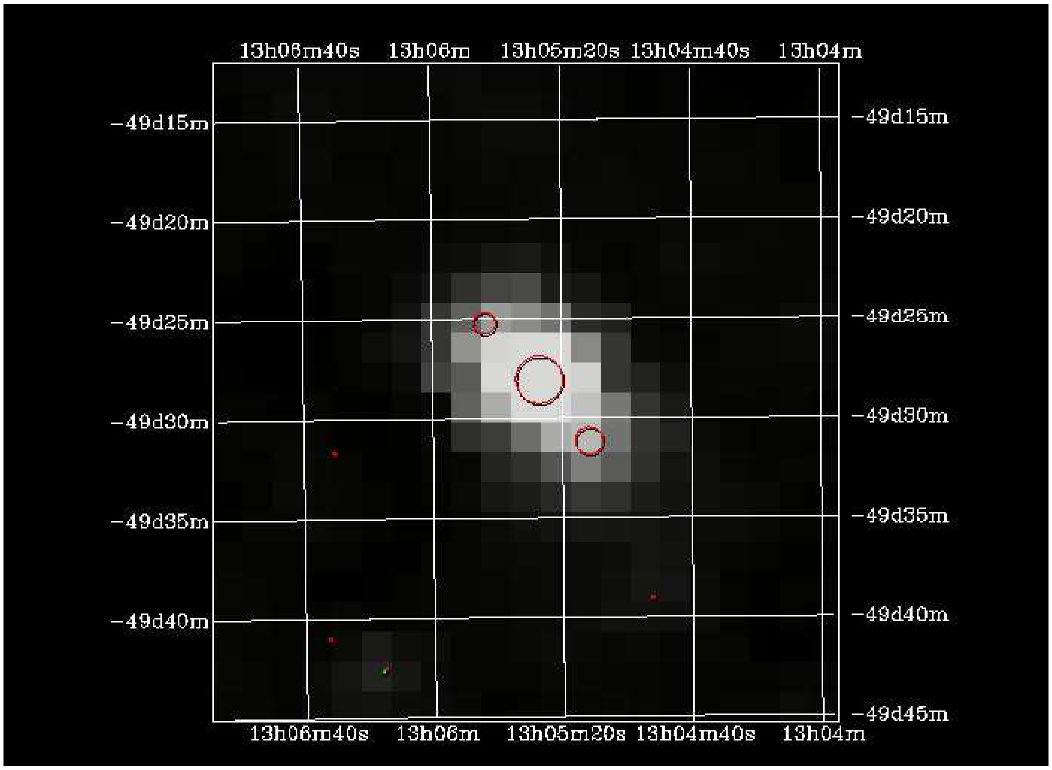

Figure 1: 12μ IRAS ISSA Image of ESO219-024.

Everton Lüdke (Santa Maria University, Departamento de Fisica, Brazil)

Kazuaki Ota (University of Tokyo, Tokyo, Japan)

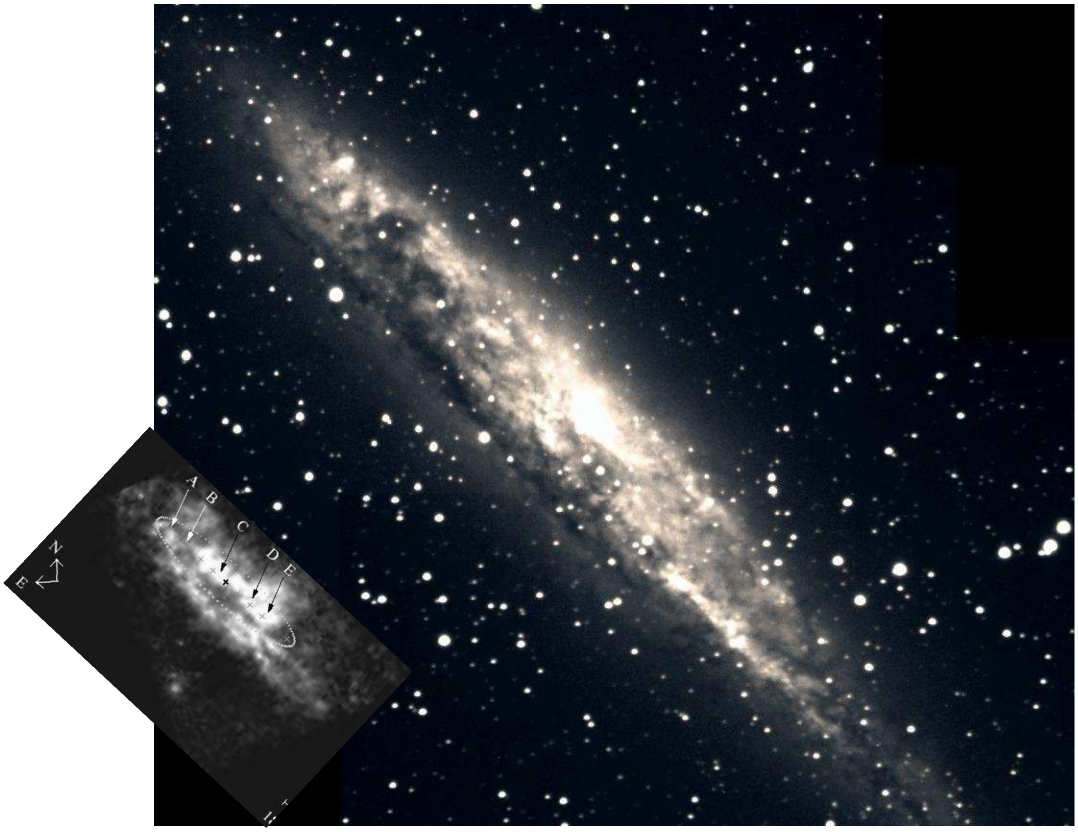

Figure 2: Optical image taken by Mike Purcell (2000), amateur astronomer. The inset is a HST/NICMOS P_α image by Marconi et al. (2000).

NAME	F(12)	F(25)	F(60)	F(100)
NGC1068(M77)	3.830e+01	8.683e+01	1.858e+02	2.405e+02
ESO219-024	3.627e+00	1.424e+01	3.881e+02	6.856e+02

$$\text{Far Infrared magnitude of ESO219-024} \approx 6$$

IRAS fluxes at 60 um and 100 um are converted in the so-called far-infrared flux according to the relation:

$$mfir = -2.5log\,(2.58f_{60} + f_{100}) + 14.75$$

shows a ridge extending above the major axis north-east of the nucleus and below the major axis to the south-west. Like the continuum the CO distribution bends towards the east at $R \sim 250''$.

Fig. 2b shows the integrated CO(2−1) spectrum for the entire region observed. The CO velocity range is about the same as for the H I in Fig. 2a. Broad peaks are present near 415, 480, 580, and 705 km s^{-1}. For an assumed symmetric system, the outer peaks would suggest a systemic velocity of 560 km s^{-1}.

Fig. 3b shows the CO(2−1) emission towards the nucleus of the galaxy. The CO covers the same velocity range as the previous spectrum. The profile shape is similar, except that the higher velocity feature is fainter than the systemic feature. In our Fig. 2 and in Fig. 5 of Dahlem et al. (1993), both features have almost the same line temperature. This likely reflects small differences (a few arcsec) in the pointing of the telescope (cf. Sect. 2.2). A fitting of gaussian components yields distinct components centred at velocities of 447, 493, 593, and 701 km s^{-1}, with a further underlying broad component centred at ∼565 km s^{-1}.

Fig. 4a shows the integrated CO(2−1) emission convolved to a resolution of 43″. Combined with corresponding SEST CO(1−0) data observed at the same resolution (Dahlem et al. 1993), the distribution of the CO(2−1)/CO(1−0) ratio is shown in Fig. 4b. The ratio varies from 0.8 to 2.0 and demonstrates that 'warm spots' with ratios larger than unity are not confined to the central region but are also observed far out in the disk. For a possible spatial correlation of these warm molecular regions with spiral arms, see Sect. 3.4.

3.2. The central region

The strong H I absorption against the central radio continuum source complicates a direct comparison of H I and CO. The H I absorption must originate from in front of the continuum whereas the CO emission may arise from in front of *and* behind the nucleus. This difference is consistent with the CO and H I lineshapes shown in Fig. 3, where the CO profile is wider than its H I counterpart at the half-maximum-intensity points. This effect must be significant: We could also plot, instead of the H I absorbing flux, the H I optical depth $\tau(\mathrm{H\,I}) = -\ln(1 + S_{\rm L}/F\,S_{\rm c})$ with F denoting the continuum source covering factor and $S_{\rm L}$ and $S_{\rm c}$ being the (negative) line and (positive) continuum flux. For F=1 the profile would resemble that shown in Fig. 3a, since the line remains optically thin even at the line centre. With $F \sim 0.25$, however, H I optical depths would be large near $V \sim 600$ km s^{-1} and the H I column density profile would become narrower. The velocity of the central CO peak lies between the velocities of the two strongest H I absorption components.

Fig. 5a shows the nuclear continuum emission at a resolution of 3.″2 in R.A. and 4.″0 in Dec. It is spatially resolved: a gaussian fit and a correction for beam size yields a source size of 7.″6 × 3.″4 (±0.″2) (correspond-

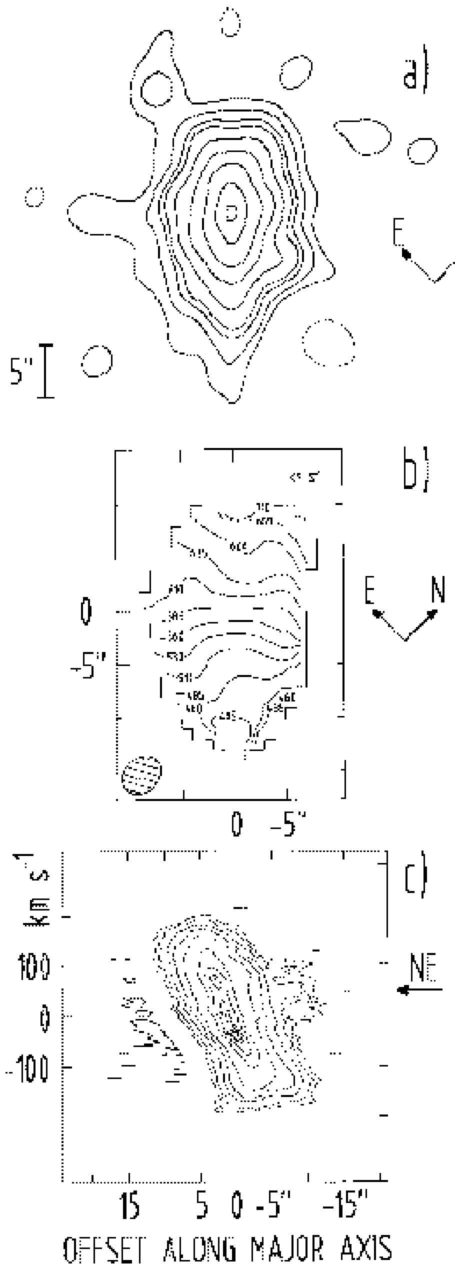

Fig. 5. The resolved nucleus at a resolution of 3.2″ in R.A. and 4.″0 in Dec. **(a)** The nuclear 1.4 GHz continuum. The contour levels have flux densities of −2 (dashed), 10, 20, 40, 60, 120, 240, 500, 1000, 1300 mJy beam^{-1}. **(b)** The LSR velocity field of the nuclear H I absorption with iso-velocity contours of 435, 460, 485, ... 685, and 710 km s^{-1}. The vertical direction is equivalent to PA = 43°. **(c)** Position-velocity diagram of the nuclear H I absorption along PA = 43° at ∼3.6″ × 7.25 km s^{-1} resolution. The velocity axis is labeled with respect to 560 km s^{-1}. Contours are -1, 1, 2,5, 10, 20, 50, 70, 85, 90, 95, 99% of the peak absorption of 612 mJy (for the peak flux density in a ∼23″ beam, see Fig. 3a).

In summary ...

- CDS coordinates RA=13h 05m 26.1s DEC=-49d 28m 15s; mag(V)=8.23;
- Best observing dates 5-26th April 2007 - one full night 12-H LST range, dark moon OK !
- Telescopes UT1, UT2, UT3 with AMBER 2.3μ, standard configuration, delay line set to 30;
- Baseline UT1-UT2-UT3 any baseline is fine for a 20-24 mas jet;
- AMBER with medium-low resolution for infrared continuum observations;
- Baseline bootstrapping;
- Visibilities well sampled during a full night observation to allow closure phase mapping and self-calibration;
- Calibrators: One quite close indeed : HD113314 (d=0.310 vis=0.986 typ=A0V)
- Full night observing run also justified for sensitivity and fringe detection limits.
- MOREOVER, it has been observed that the AGN of ESO219-024 is heavily absorbed by dust and we will need other tools with ALL available UT telescopes. Better still, WE SHOULD WAIT for the experts ...

Thanks for the lovely meeting !!!!

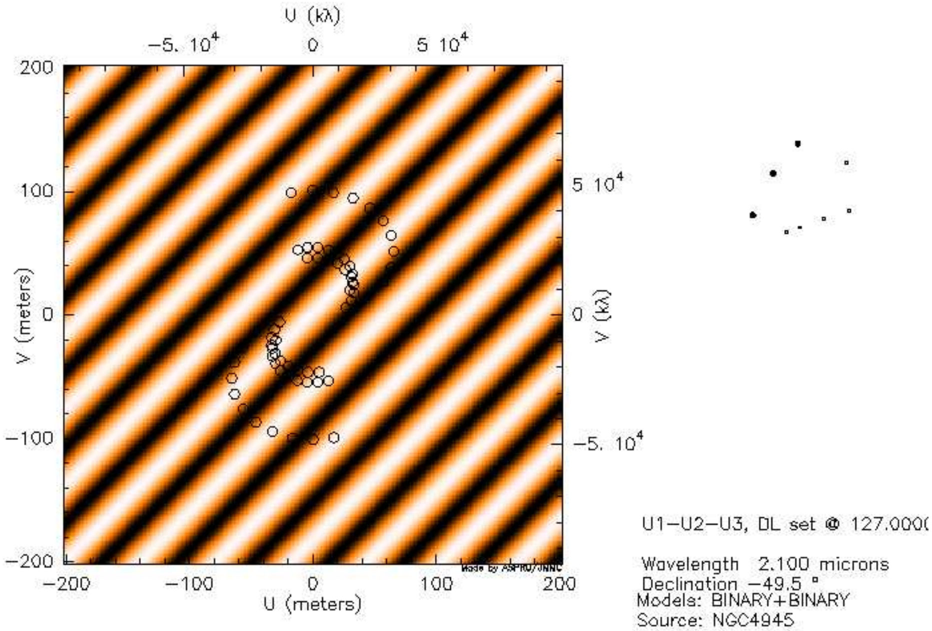
U (kλ)
−5. 10^4
0
5 10^4
V (meters)
V (kλ)
U (meters)
Made by ASPRO/JMMC
U1−U2−U3, DL set @ 127.000(
Wavelength 2.100 microns
Declination −49.5 °
Models: BINARY+BINARY
Source: NGC4945

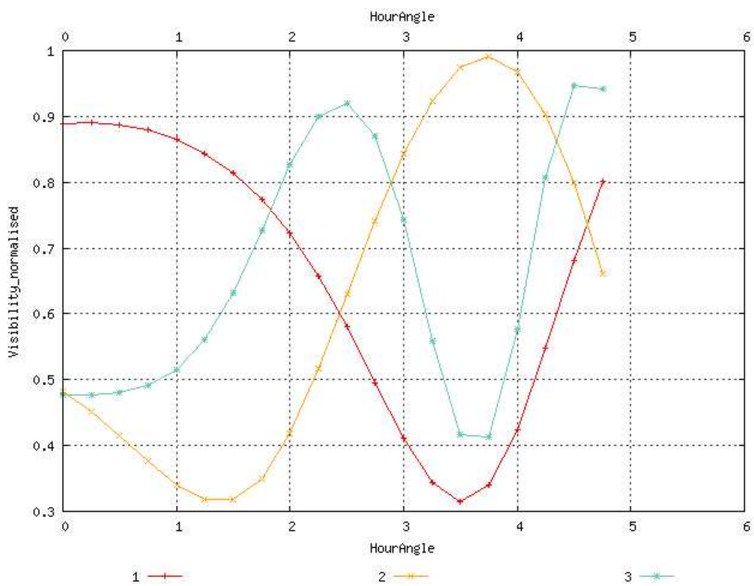
HourAngle
Visibility_normalised
HourAngle
1
2
3

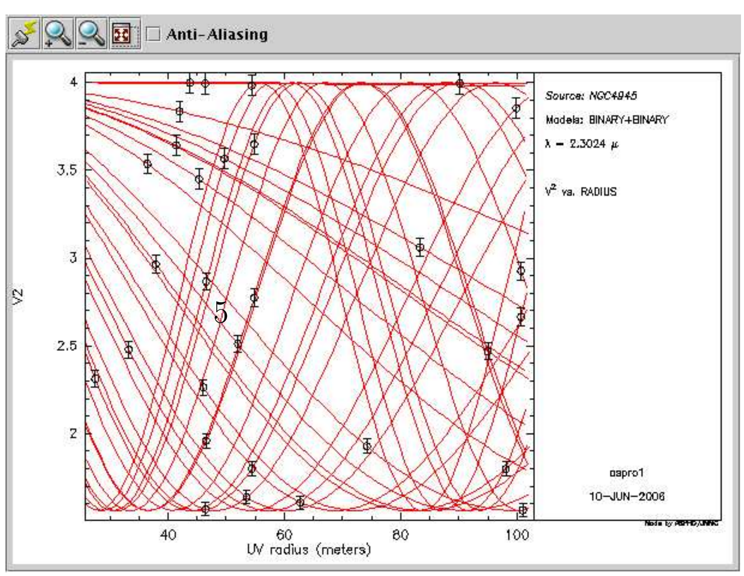
Anti-Aliasing
V2
UV radius (meters)
Source: NGC4945
Models: BINARY+BINARY
λ = 2.3024 μ
V² vs. RADIUS
aspro1
10-JUN-2006
Made by ASPRO/JMMC